



## Bulge Formation of a Buoyant River Outflow

Robert J. Chant,<sup>1</sup> Scott M. Glenn,<sup>1</sup> Elias Hunter,<sup>1</sup> Josh Kohut,<sup>1</sup> Robert F. Chen,<sup>2</sup>  
Robert W. Houghton,<sup>3</sup> Jen Bosch,<sup>1</sup> and Oscar Schofield<sup>1</sup>

Received 10 January 2007; revised 1 June 2007; accepted 28 September 2007; published 24 January 2008.

[1] Observations taken during the Lagrangian Transport and Transformation Experiment (LaTTE) in 2005 indicated that the Hudson's river outflow formed a bulge of recirculating fluid that limits the volume of fresh water that is advected away in a coastal current. Focusing on an event that began with downwelling winds we made estimates of the fresh-water flux in the coastal current and the fresh water inventory of the bulge. The coastal current was characterized by a surface advected plume in thermal wind balance. However, the freshwater transport in the coastal current was less than 1/2 of the total freshwater outflow. The bulge extended 30 km from the coast and 40 km in the along-shore direction and was evident in ocean color imagery. Recirculation in the bulge region was also apparent in daily averaged surface current radar data, but this flow pattern was obscured in the hourly data by tidal and wind-forcing even in the diurnal band. Nevertheless, many aspects of the Hudson's outflow are consistent with recent laboratory experiments and numerical simulations of buoyant discharges. The growing bulge transports the river's outflow to the head of the Hudson shelf valley where it crosses the 50 m isobath. Previous work in this region indicates that frontal features reside along this isobath. We observed fresh water being transported along this isobath and is suggestive of a rapid cross-shelf transport pathway for fresh water. Both the bulge formation and cross-shelf transport have significant biogeochemical implications.

**Citation:** Chant, R. J., S. M. Glenn, E. Hunter, J. Kohut, R. F. Chen, R. W. Houghton, J. Bosch, and O. Schofield (2008), Bulge Formation of a Buoyant River Outflow, *J. Geophys. Res.*, 113, C01017, doi:10.1029/2007JC004100.

### 1. Introduction

[2] The classic model of fresh water debouching into the ocean has the outflow deflected to the right (in the northern hemisphere) and forming a narrow coastal current that is trapped within a few internal Rossby radii of the coast [Garvine, 1999]. The coastal current can be either surface advected or bottom attached [Yankovsky and Chapman, 1997]. In the absence of wind and wave forcing (Fewings et al., Observations of Cross-Shore flow driven by cross-shore winds on the inner continental shelf, submitted to *Journal of Physical Oceanography*). Cross-shelf transport in bottom attached coastal currents is primarily contained in a bottom Ekman layer [Chapman and Lentz, 1994]. However, at a critical depth the offshore Ekman transport is shut down by baroclinic forcing and the plume is trapped to an isobath [Chapman and Lentz, 1994; Yankovsky and Chapman, 1997]. For surface advected plumes the width is set by the internal Rossby Radius [Lentz and Helfrich, 2002] which is typically on the order of a few km in the coastal

ocean. In general, these models emphasize that in the absence of winds coastal current dynamics severely limit cross-shelf transport of buoyant water on continental shelves.

[3] Buoyant outflows may also contain a bulge-like region in the vicinity of the outflow, and the cross-shelf extent of these bulges can be many times the width of the down stream coastal current. Yankovsky and Chapman [1997] incorporated a bulge in a steady state model which they closed by equating the buoyancy flux in the coastal current to the buoyancy flux exiting the estuary. With this steady state assumption they developed an elegant theory that related coastal current structure to estuarine discharge rate and the cross-shore bathymetric slope.

[4] Recent modeling and laboratory studies of buoyant outflows have provided a more detailed characterization of bulge structure [Avicola and Huq, 2003a; Fong and Geyer, 2002; Horner-Devine et al., 2006] and emphasize that a bulge may be *unsteady* and grow in time. Consequently, the fresh water flux out of the estuary ( $Q$ ) is greater than the fresh water flux in the coastal current ( $Q_{cc}$ ). In a series of numerical experiments Fong and Geyer [2002] found that  $Q_{cc}/Q$  was inversely proportional to a Rossby number with  $Q_{cc}/Q$  dropping from 0.65 to 0.4 as the Rossby number increased from 0.1 to 1. In the laboratory Avicola and Huq [2003b] reported that only approximately 1/3 of the outflow became incorporated in the coastal current, with the rest of the outflow going into bulge formation. Fong and Geyer

<sup>1</sup>Institute of Marine and Coastal Studies, Rutgers University, New Brunswick, New Jersey, USA.

<sup>2</sup>University of Massachusetts Boston, Massachusetts, USA.

<sup>3</sup>Lamont-Doherty Earth Observatory, Columbia University, Palisades, New York, USA.

[2002] discussed the mechanisms by which the bulge feeds the coastal current by invoking a model by *Nof and Pichevin* [1988] where the amount of fresh water entering the coastal current is determined by the amount of the eddy (bulge) pinched off at the coastal wall. As the Rossby numbers increases the eddy's center moves increasingly further from the coastal wall and reduces the fraction of the eddy that is pinched off and thus diminishes the freshwater transport into the coastal current.

[5] *Avicola and Huq* [2003a, 2003b] discuss bulge formation in terms of the angle that the outflow makes with the coastal wall (outflow angle) and the angle that the discharge impacts the coast (impact angle). They note that these two angles are related, with oblique outflow angles corresponding to oblique impact angles while outflows that normal to the coast lead to flows that impact the coastal wall at right angle. *Avicola and Huq* suggest that the physics of bulge formation is determined by the angle that the outflow impacts the coast, and that this impact angle is determined by the outflow angle. For oblique impact angles a coastal current forms. Bulge recirculation increases as the impact angle approaches 90 degrees. Laboratory experiments by *Horne-Devine et al.* [2006] show even more dramatic shunting of coastal current by bulge formation as the recirculation completely pinches off the coastal current and the entire outflow goes into bulge formation.

[6] Wind-forcing also plays a critical role in the cross-shelf transport of river plumes [*Whitney and Garvine*, 2005]. Modeling studies [*Fong and Geyer*, 2002] reveal that upwelling winds are effective both in transporting river plumes offshore and in entraining the plume into the coastal ocean. Observational studies of coastal currents reveal that the structure of the flow and salt field [*Rennie and Lentz*, 1999] and diapycnal fluxes [*Houghton et al.*, 2004] appear to be consistent with numerical studies [*Fong and Geyer*, 2001]. Despite this there has been little research on the effect of wind-forcing on bulge dynamics with the notable exception of *Choi and Wilkin* [2007].

[7] In this study we present data from the Hudson River plume that was collected as part of the LaTTE '05 (Lagrangian Transport and Transformation Experiment) field effort between March and May 2005. LaTTE is focused on the transport and transformation of dissolved and suspended materials such as nutrients, contaminant metals, Colored Dissolved Organic Matter (CDOM) and carbon from this highly urbanized estuary. The Hudson's outflow mixes with the outflow from the Passaic and Raritan River (Figure 1) plus an additional 100 m<sup>3</sup>/s of treated sewage and enters the coastal ocean near Sandy Hook. Once beyond Sandy Hook there is no clear channel to steer the plume. However, 10 km to the east resides the head of the Hudson Shelf Valley (Figure 1) which bisects the entire 150 km wide New York Bight Shelf. The Hudson Shelf Valley was formed by the ancestral Hudson River and its formation may have been augmented by catastrophic flooding following the drainage of the late Wisconsin glacial lakes [*Newman et al.*, 1969]. Recent analysis of near-bottom currents meter data in the shelf valley suggests that it may provide an important conduit for cross-shelf exchange [*Harris et al.*, 2003].

[8] The first order fate and transport of dissolved and suspended material in the Hudson Plume depends on the transport pathway of the fresh water. If the outflow forms a

coastal current, transport pathways will be limited in the cross-shelf direction. However, if bulge formation dominates, both the ballooning of the outflow and the limited down-shelf advection would radically alter transport pathways. Furthermore, if bulge formation brings the outflow into the vicinity of the Hudson shelf valley ambient circulation associated with the shelf valley [*Harris et al.*, 2003] could significantly drive cross-shelf transport pathways. In this paper we demonstrate that the Hudson's outflow is in fact highly susceptible to bulge formation and that this allows the outflow to rapidly mix across the 100 km wide New York Bight.

## 2. 2005 Field Effort

[9] The LaTTE program is an interdisciplinary process study of the Hudson River plume conducted within a sustained coastal ocean observatory. The observatory was designed, built and operated by the Rutgers University Coastal Ocean Observation Lab [*Glenn and Schofield*, 2004]. Observational components include a pair of satellite direct-broadcast data acquisition systems for tracking the international constellation of ocean color and thermal infrared imaging satellites, a triple-nested multistatic CODAR High Frequency (HF) Radar network for surface current mapping, and a fleet of autonomous underwater gliders for subsurface mapping of water properties. An operations center controls the observatory data acquisition, aggregates the data, and produces data products and forecasts to provide a spatial and temporal context for process studies and adaptive sampling. The LaTTE 2005 study included a mooring array that was deployed for approximately 2 months and shipboard surveys.

[10] The shipboard surveys occurred between 9 April and 22 April 2005 with the R/V Cape Hatteras and R/V Oceanus. The cruise featured two Rhodamine dye studies with dye injected on 11 April and 18 April in the surface layer in the vicinity of Sandy Hook. The Cape Hatteras was used to track the dye which was done with a towed undulating vehicle and an instrument package located 1–2 m below the surface that was mounted to a pole over the starboard side of the ship. Instrumentation aboard the undulating vehicle and on the over-the-side mount included a CTD, OBS and fluorometers for Rhodamine dye, Chlorophyll-a and CDOM. In addition the over-the-side mount included a 1200 kHz RDI ADCP. During the dye injection a pair of surface drifters with drogues covering the top two meters of the water column was deployed. The Oceanus was used primarily for biological sampling. During the cruise broadband and cell phone Internet connectivity aboard the two research vessels enabled communications between the ships and the operations center for coordinated adaptive sampling with the research vessels and gliders.

[11] Satellite data from the U.S. (AVHRR, MODIS), India (Oceansat) and China (FY1-D) acquired by the two ground stations was processed using both SeaSpace and NRL algorithms [*Lee et al.*, 2002]. The nested CODAR HF Radar networks are operated at 25 MHz, 13 MHz, and 5 MHz. Radial current data from each site is processed as described by [*Kohut and Barrick*, 2001]. Radial data from the 25 MHz sites is combined into total vector maps using the algorithm described by *Kohut et al.* [2006] and includes

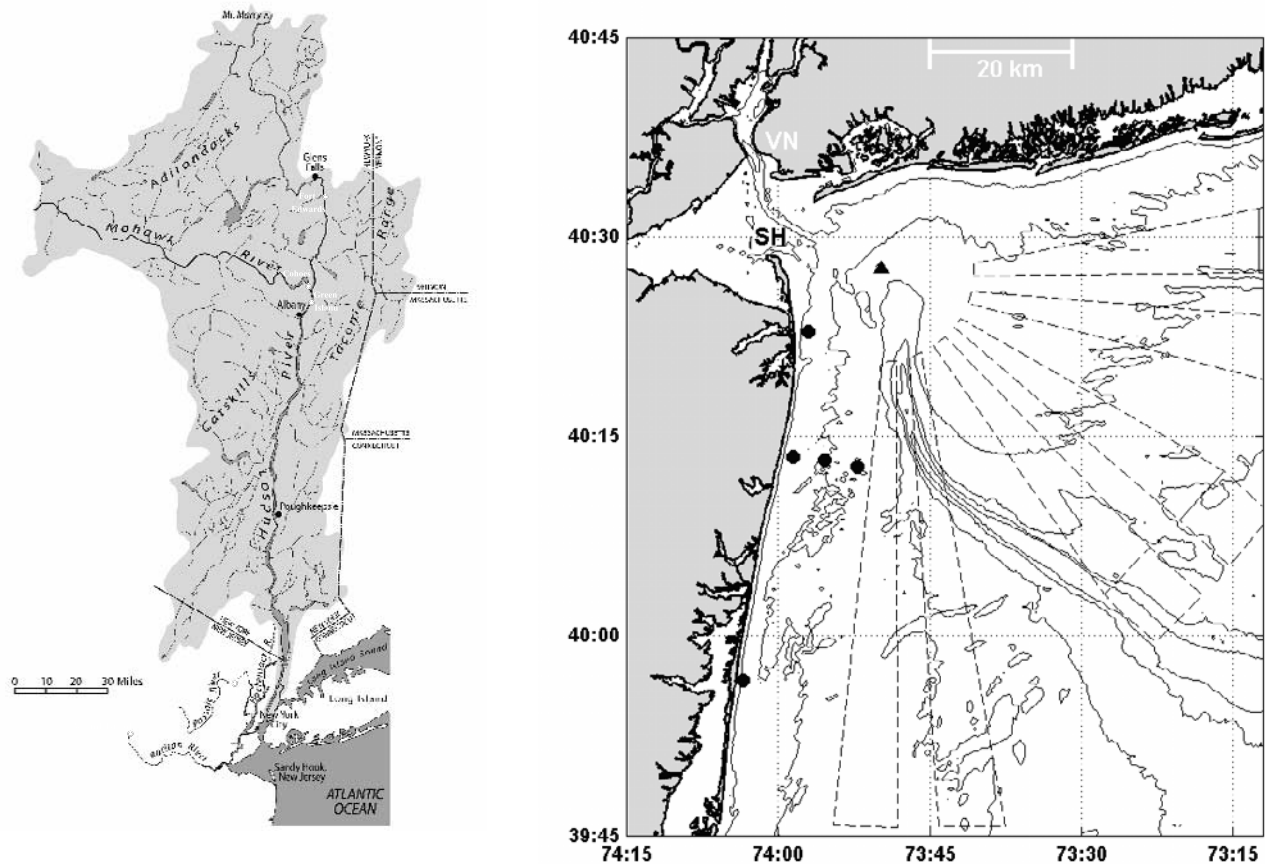


**Figure 1.** Study area. Left panel shows water shed and USGS gauging stations at Bound Brook, Little Falls, Cohoes, Fort Edwards and Green Island and location of USGS ADCP in Poughkeepsie. Right panel depict mooring locations as filled black circles. Contours are at 10 meter intervals. Black triangle shows location of Ambrose light tower. The straight to the west of VN is the Verrazano Narrows, and the peninsula immediately east of SH is Sand Hook. The deep channel cutting across shelf is the Hudson shelf valley.

the calculation of the Geometric Dilution of Precision (GDOP) criteria based on the actual radial data used in each individual map. The resulting quality controlled maps are produced every half hour with a spatial resolution of 1.5 km. Glider data is acquired every time the glider surfaces, which in LaTTE was typically every 3 h. The CTD on the glider operates at 0.5 Hz and yields a vertical resolution of 0.25 m. The glider's SeaBird CTD data is processed using the correction for the response time of both the temperature sensor and conductivity sensor and the thermal lag associated with flushing of conductivity cell [Morison *et al.*, 1994] with the coefficients set by minimizing the upcast/downcast salinity profile differences from summertime data collected on the New Jersey continental shelf.

[12] The moorings consisted of a five element array deployed from 18 March to 19 May 2005 (Figure 1), each containing a Doppler current meter and Conductivity/Temperature (CT) sensors. The four northern moorings were outfitted with CT sensors 50 cm above the bottom (mab) and at 1 and 7 m below the surface (mbs). The southern mooring had surface and bottom CT sensor. The central mooring was damaged, likely due to barge traffic, causing the complete loss of data from the surface and middle CT

sensor. We also utilized Doppler current profile data from a NOAA's PORTS mooring in the Verrazano Narrows and from a USGS mooring in the Hudson River at Poughkeepsie, New York (Figure 1). During this experiment the Poughkeepsie ADCP was in the fresh-water part of the river. The Poughkeepsie Doppler data was calibrated by USGS so that the data could be used to estimate volume transport. Wind data was obtained from the NOAA station at Ambrose Light, and river discharge data was obtained from USGS gauges in the Mohawk River in Cohoes, the Hudson at Fort Edwards, the Passaic at Little Falls and the Raritan at Bound Brook (Figure 1). Throughout the manuscript we use the orientation of the New Jersey coast to characterize winds as upwelling (winds from the south) or downwelling (winds from the north).

### 3. River Discharge

[13] Essential to the analysis in this paper is an estimate of the discharge of fresh-water into the coastal ocean which requires estimates of fresh water fluxes from the ungauged portions of the watershed. The Hudson dominates the fresh water fluxes and has a mean April discharge of  $1100 \text{ m}^3/\text{s}$

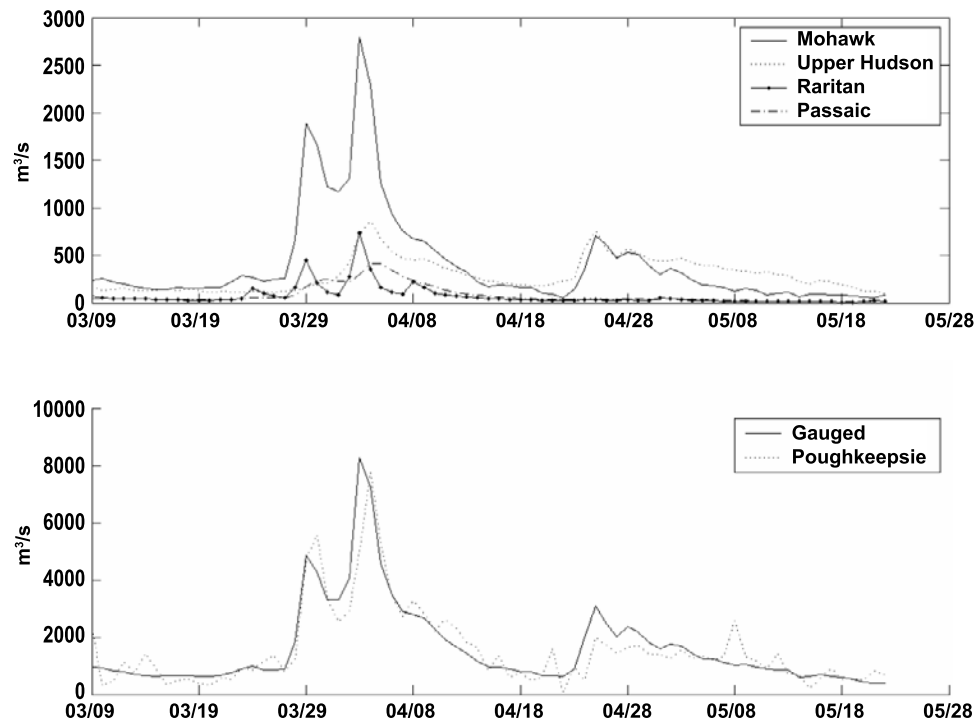


**Figure 2.** Upper panel shows discharge from USGS gauging stations. Lower panel shows two estimates of total discharge as discussed in text.

based on a 47-a record at Green Island. The Passaic and Raritan rivers mean April flows are  $57 \text{ m}^3/\text{s}$  and  $49 \text{ m}^3/\text{s}$  respectively based on nearly 100 a of discharge data. Unfortunately the Green Island gauge is no longer operational and discharge must now be estimated by the sum of upstream gauges in the Mohawk at Cohoes and upper Hudson at Fort Edwards. The watershed area at Green Island is 1.3 times the combined area of the Cohoes and Fort Edwards watershed so we assume that discharge rate at Green Island is equal to 1.3 times the sum of Cohoes and Fort Edwards. The 1.3 factor is also found in a regression of overlapping discharge records that extend from 1979–1998 (not shown). Downstream of Green Island the additional watershed increases discharge by another 60% [Abood, 1977; Lerczak *et al.*, 2006]. Thus we estimate the total Hudson’s discharge as twice the sum (i.e.,  $1.3 * 1.6$ ) of Cohoes and Fort Edwards plus the measured discharge from the Passaic and Raritan rivers. We refer to this estimate as the “gauged” estimate of river discharge. Discharge from sewage outflows were not included in this estimate because some fraction of the regions water supply is drawn from the river down stream of the USGS gauges.

[14] The hourly transport estimates at Poughkeepsie were filtered with a Lancocz filter with a cut-off period of 32 h to remove tidal period variability. We note that in addition to river discharge this record also contains additional transport associated with local and remote meteorological forcing [Lerczak *et al.*, 2006]. This is apparent in the noisier nature of the Poughkeepsie data relative to the gauged data. However, this additional transport is relatively small and its value diminishes over longer averaging periods. The watershed upstream of Poughkeepsie contains 89% of the Hudson’s total water and thus our “Poughkeepsie” estimate of river discharge is 1.12 times the filtered Poughkeepsie

transport estimate plus the gauged measurements in the Passaic and Raritan Rivers. Figure 2 compares our “gauged” discharge estimate with the “Poughkeepsie” estimate. In general the estimates agree well, with the Poughkeepsie estimate generally slightly lower than the gauged estimate, though not always. Between 1 March and 1 June the mean from the gauged estimate was  $1524 \text{ m}^3/\text{s}$  while the mean value of the Poughkeepsie estimate was  $1466 \text{ m}^3/\text{s}$ . The Poughkeepsie estimate was even higher during the time period that this paper focuses on. Between April 8th and 14th the mean flow using the gauged data was  $1981 \text{ m}^3/\text{s}$ , while using estimates using the Poughkeepsie data was  $2385 \text{ m}^3/\text{s}$ . Some of this discrepancy may be due to variations in the distribution of snow cover and precipitation across the watershed during this time, which if true implies that the Poughkeepsie measurement would be more accurate. However, the difference may also reflect uncertainties in the USGS calibration. Thus we will use these two values as bounds for the estimates the total river discharge. The gauged discharge estimate peaked on 3 April at  $8290 \text{ m}^3/\text{s}$  while the Poughkeepsie estimate peaked on 4 April at  $7825 \text{ m}^3/\text{s}$ . Also during the peak flows the estimate at Poughkeepsie lags the gauged estimate by one day. We note that peak discharge in all of the gauged rivers in the system were significantly above typical peak flows. For example, the discharge at Cohoes, the gauge with the largest flow, peaked at  $2789 \text{ m}^3/\text{s}$  and represents the 8th largest discharge to date in the 88-a record.

#### 4. Estuarine Outflows

[15] Filtered depth averaged velocities from the ADCP at the Verrazano Narrows increase within a few days of the discharge peaks (Figure 3). However, the lag time between

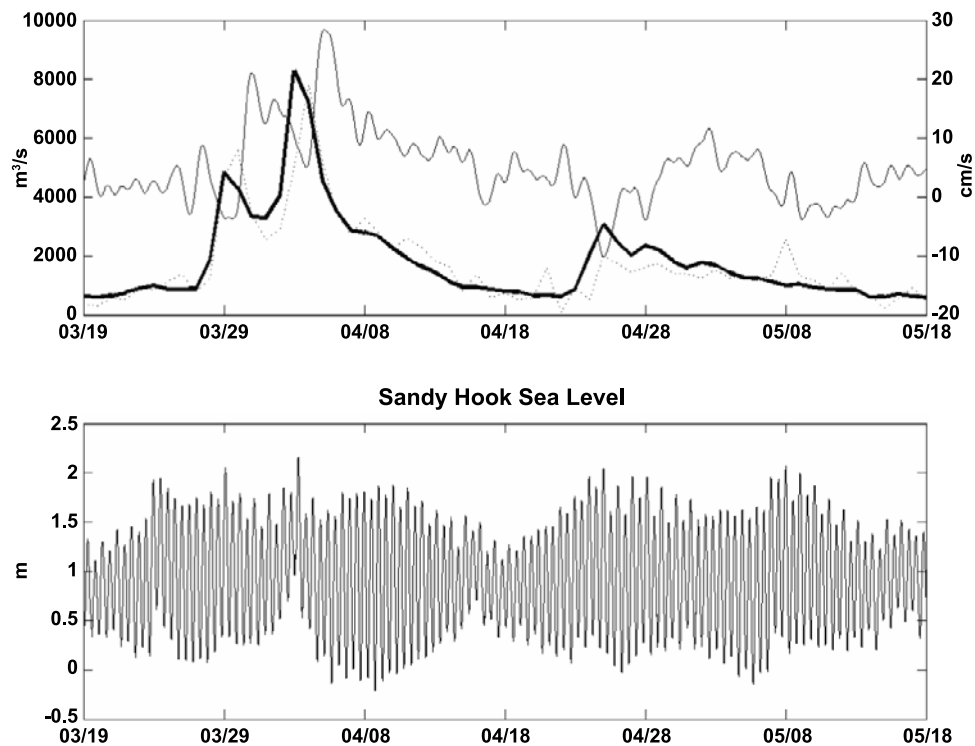


**Figure 3.** Upper panel shows “Gauged” estimate of total discharge (thick line), “Poughkeepsie” discharge estimate (dotted line), low-pass filtered depth averaged flow from Verrazano Narrows (thin line). Lower panel depicts sea level at the Battery as recorded by NOAA tide gauge.

discharge at the upstream gauges and the outflow at the Narrows is variable and is impacted by wind-forcing and the spring neap cycle. It should be noted that the mooring at the Verrazano is on the flank and likely is a better reflection of the upper layer transports than barotropic flows. Filtered velocity at the Narrows lagged the two large peaks in discharge in late March and early April by 2 days. A longer lag time of nearly 1-week was evident following the smaller peak in late April. Here the river peaked on 25 April while the outflow at the Narrows peaked during the neap tide around 2 May. The correlation between the gauged data and the outflow at the Verrazano narrows had a peak value of 0.75 at a two day lag.

[16] During the peak discharge in early April upwelling favorable winds (Figure 4) between 6–8 April drove the plume to the east along the Long Island coast and drove upwelling along the New Jersey Shelf. The eastward transport of the plume is clearly evident in numerous satellite imagery, such as absorption at 448 nm [Lee *et al.*, 2002] (Figure 5). During this period surface salinities at the moorings are low, but begin to rise as the upwelling winds persist. By the end of this upwelling event on April 8th surface salinities at all of the mooring sites increased to over 30 psu (Figure 6).

[17] On 8 April winds shifted to downwelling favorable and were modulated significantly by diurnal variability. Following the shift to downwelling winds a frontal passage was evident in the surface salinity on 8 April at N1 and C1 and 9 April at S1 (Figure 6a). On the basis of the timing of the frontal passage past C1 and S1 the front propagates down-shelf at 0.69 m/s which is faster than estimates of the

internal wave speed  $(g'h)^{1/2}$  of 0.50 m/s, suggesting that the downwelling favorable winds increased the down-shelf propagation. However, while rapid down shelf currents were evident at C1 and S1, currents at N1 were weak and generally upshelf (Figure 6b). Furthermore, currents near the surface (the top ADCP bin) at C2 and C3 were weak and the salinity (at C3) was high suggestive that these moorings were seaward of the coastal current. There was, however, a slight freshening on 4/11 and 4/12 in the surface at the C3 in response to the diurnal wind variability.

[18] Images obtained from nearly simultaneous passages of Oceansat (17:09 GMT) and MODIS (17:13 GMT) on 4/9 revealed that the coastal current width diminishes as it propagated south. At the central mooring array it is approximately 3 km wide while at S1 its width is closer to 2 km. Strong down-shelf currents were apparent in low-pass filtered currents at inner moorings at S1 and C1, while the two offshore moorings along the C-line were seaward of the plume and currents were weak. Currents were also weak at N1, despite the relatively fresh and buoyant water at the surface. The bulge was also evident in the satellite imagery and surface currents from CODAR showed enhanced currents along its seaward edge. Furthermore, the data shown in Figure 7 suggests a region of recirculation centered approximately halfway across the bulge, unfortunately, because of the geometry of the CODAR array we cannot obtain surface current vectors on the shoreward side of the bulge. On the basis of the radius of flow curvature ( $\sim 7$ – $10$  km) and filtered surface current speeds (30 cm/s) the Rossby number is in the range of 0.3–0.5.

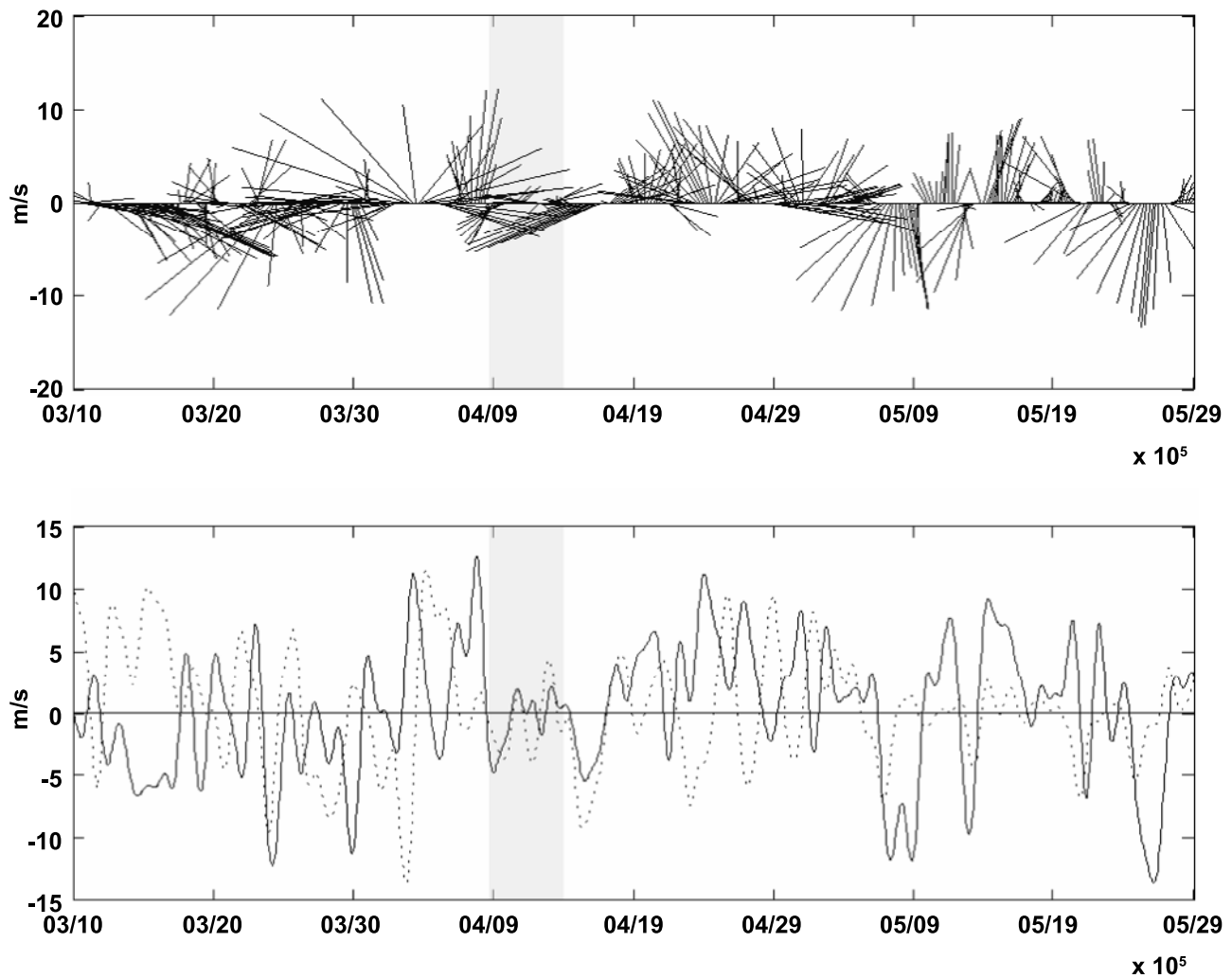


**Figure 4.** Low-pass filtered winds from Ambrose tower. Wind sticks (upper panel) and north(+)/south(−) (solid) and east(+)/west(−) (dashed) winds (lower panel). Gray area in both panels indicate time period of bulge growth focused on in this paper.

[19] Satellite images (Figure 7) resolved the remains of the earlier plume that was transported to the east along the LI coast on 6–8 April by winds from the south. This remnant plume was evident as a broad region of enhanced absorption that extended 60–70 km east of Sandy Hook and 50 km offshore. Shipboard survey confirmed that this region was indeed associated with a fresh water plume and that it was isolated from the newly formed coastal current by the saline surface waters over the Hudson shelf valley.

[20] Following the initial pulse of downwelling favorable winds on 8–9 April a strong sea-breeze developed with peak upwelling favorable winds occurring late each day. The amplitude of the diurnal wind-forcing was approximately 10 m/s. The strong sea-breeze forcing persisted though 4/14. Despite the strong diurnal variability filtered winds have a near zero average between 10 April and 14 April (Figure 6c). Current speeds in the coastal current generally decreased during this time and began to oscillate with the sea-breeze forcing by 4/11. By 4/13 the coastal current was shut down despite the presence of significant buoyancy and the lack of persistent upwelling winds.

During this period of weak low-frequency winds (4/10–4/14) the outflow ballooned into a large bulge of fluid of 20–25 psu and 5–7 m thick that remained in the vicinity of the New York Bight Apex. To determine the fraction of fresh water that goes in to bulge formation and the fraction that is advected away in the coastal current we compare both estimates of river discharge to estimates of fresh-water flux in the coastal current and the fresh water content of the bulge.

## 5. Coastal Current Fresh Water Transport

[21] With the moored, shipboard and satellite imagery we made estimates of the fresh water transport of fresh water in the coastal current. Salinity data from the 3 CT sensors at C1 were linearly interpolated in the vertical to coincide with each of the ADCP bins. Salinity above the surface CT sensor was assumed to be constant. Missing velocity data in the top  $\sim 1.5$  m of the water column, due to acoustic sidelobe interference with the surface, were filled by extrapolating the profile to the surface. The extrapolation first calculates the vertical shear in the top 1 m of the profile and

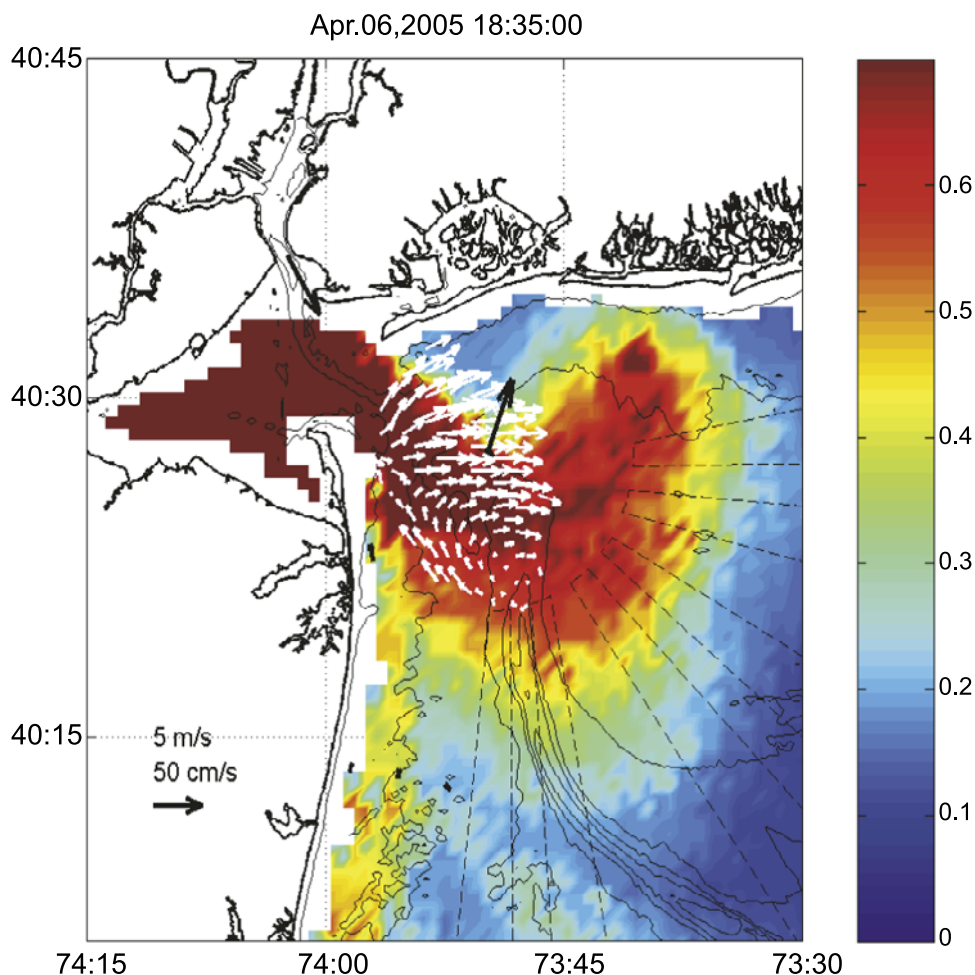


**Figure 5.** Color shows absorption at 488 nm from MODIS using algorithm from *Lee et al.* [2002]. Red indicates high absorption, blue is low absorption. White vectors show CODAR low-pass filtered currents. Filtered winds from Ambrose light tower is represented by black vector in middle of CODAR field. Black arrow depicts the filtered surface currents from moored ADCP's. Isobaths are contoured at 10m intervals. The scale arrow is for current speed (50 cm/s) and wind speed (5 m/s).

assumed that this shear decreases linearly to zero at the surface. With the extrapolated velocity ( $v$ ) and interpolated salinity profile ( $s$ ) the fresh water flux of the coastal current per unit width ( $FW_{cc}$ ) was estimated as

$$FW_{cc} = \int_{z_1}^{\eta} v(z) \times (S_a - s(z)/S_a) dz$$

where  $z_1$  is the depth of the first ADCP bin,  $\eta$  is the sea surface elevation and  $S_a$  is the ambient salinity on the inner shelf, which we set to equal to the salinity at C1 prior to the frontal passage on 8 April (30.6 psu). We note that the bottom salinity sensor had serious fouling and experienced significant drift over the 2 months deployment. While this drift was probably not constant we attempted to correct for it by removing the mean drift. Nevertheless salinities appear to remain erroneously low as evidenced by the salinity (and density) inversions that occurred between the bottom and mid-depth CT sensors during this record (not shown). While this error tended to produce an overestimate of the freshwater flux, down-shelf velocities tended to be weak below 7 m depth and thus this error is likely to be small.

[22] Estimates of fresh-water flux per unit width are shown in Figure 8. Fresh water flux peaked after the passage of the evening pulse on the 9th at slightly over  $0.6 \text{ m}^2/\text{s}$ , and was followed by a series of pulses. The initial pulses occur at the semi-diurnal period but become significantly modified by wind-forcing that is predominantly at the diurnal period. During the first 48 h after the passage of the coastal current fresh water flux is between 0.2 and  $0.6 \text{ m}^2/\text{s}$  with oscillations at both diurnal and semi-diurnal periods. After 4/11 the sea breeze forcing intensifies and the down-shelf transport of fresh water is shutoff on the mornings on 4/11 and 4/12. During this time diurnal fluctuations in the wind lead those in the fresh water flux by about 8 h. Between 4/13 and 4/15 the coastal current stalls and fresh water flux goes to zero, despite the fact that winds have a near zero daily mean. Finally on 4/15–16 an east-northeasterly wind dramatically increased fresh water fluxes to over  $0.8 \text{ m}^2/\text{s}$ .

[23] Fresh water flux in the coastal current,  $Q_{cc}$ , is estimated by multiplying  $FW_{cc}$  by the width of the plume. Both satellite imagery (Figure 7) and shipboard observations (Figure 9) indicate that the plume's width is approx-

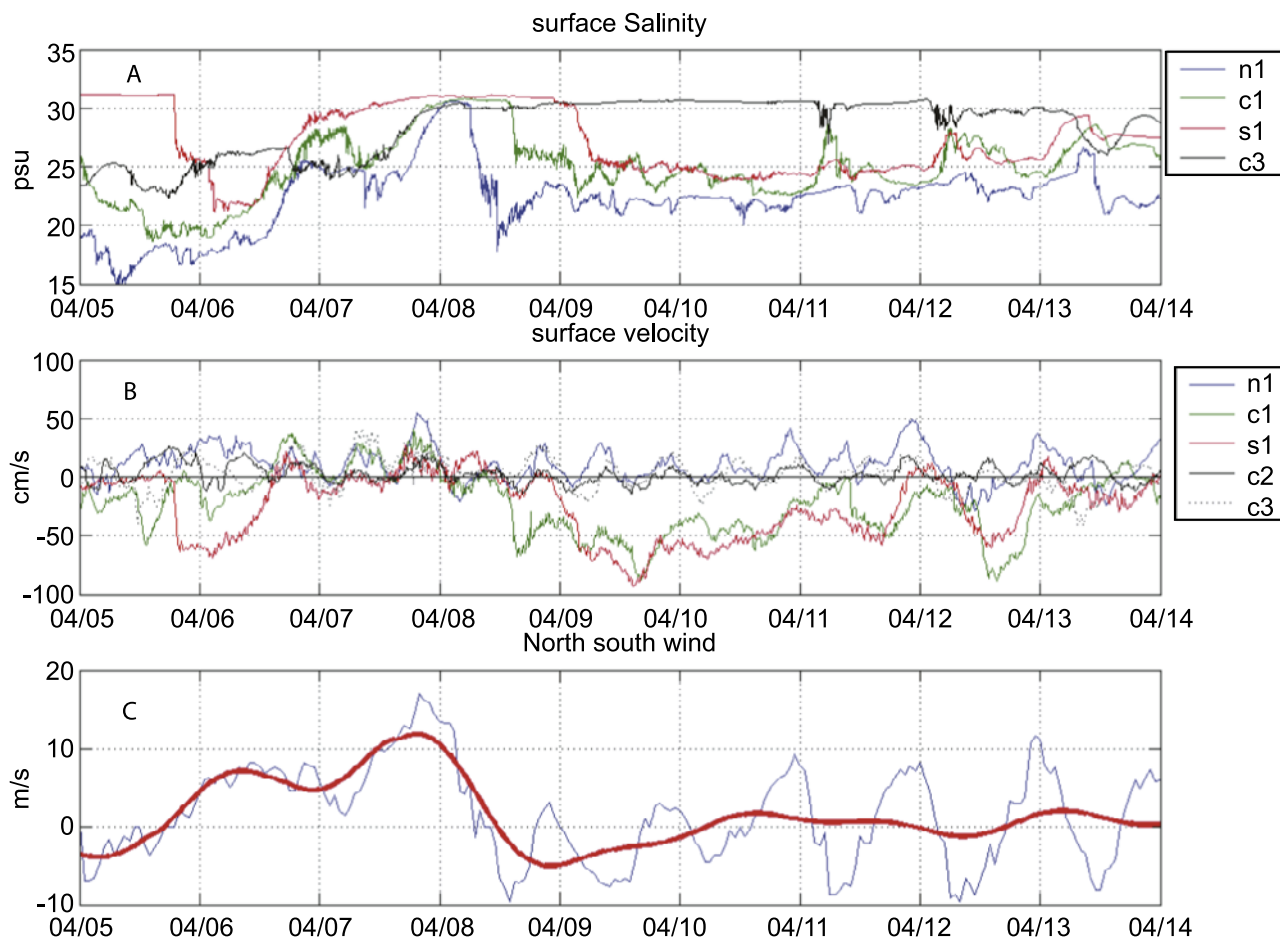


**Figure 6.** Surface salinity from mooring array (upper panel). Hourly surface along shore currents from mooring array (middle panel). Hourly (blue) and low-pass filtered (red) North/south winds from Ambrose light tower (lower panel).

imately 3 km and yields a water flux of  $\sim 800 \text{ m}^3/\text{s}$  which is significantly smaller than the mean discharge out of the estuary. A plume with a width of 3 km is also consistent with the lack of any significant down-shelf flows during this time period from the ADCP mooring at C2 that lies 4 km from the coast. We also estimated  $Q_{cc}$  assuming that the vertical shear remained constant above the top good ADCP bin. These results were nearly identical to those presented above.

[24] A nearly identical estimate of fresh water flux was obtained with a crossing of the coastal current around 1200 GMT on 10 April. The timing of this transect is indicated by the vertical line in Figure 8, while the location of the transect is shown in Figure 7. During this crossing the estimate of the fresh water from the moorings was  $0.29 \text{ m}^2/\text{s}$ , corresponding to a fresh water transport of approximately  $1000 \text{ m}^3/\text{s}$ . Like the moored data the shipboard data needed to be extrapolated to the surface, which we did assuming the shear remained constant to the surface. This extrapolation method differs than the one we applied on the moored velocity data, where we let the shear go to zero at the surface, because the shipboard data is missing the top 3.0 m of the water column and the moored data suggests that the shear remains relatively constant between 3.0 mbs and 1.0 mbs. While vertical shear may weaken near the surface, assuming

it to be constant yields an *overestimate* of the fresh-water flux. The shipboard data clearly shows that the plume is surface advected and 3–4 km wide (Figure 9a) and  $\sim 5 \text{ m}$  thick. Freshwater transport per unit width exceeds  $0.3 \text{ m}^2/\text{s}$  about 1 km from the shore and decreases both landward and seaward of this point and the total freshwater flux is approximately  $780 \text{ m}^3/\text{s}$ .

[25] Finally a third estimate of the fresh water flux was obtained using the density field and following the geostrophic arguments of *Fong and Geyer* [2002]. *Fong and Geyer* [2002] found that the fresh water transport in their modeled coastal current was linearly proportional to  $(g'h)^2$  where  $g'$  is estimated with the mean density in the plume and  $h$  the mean thickness. They found that freshwater transport was equal to  $\gamma \frac{\rho(g'h)^2}{g\beta S_0 f}$ , where  $\beta$  is saline expansivity ( $\beta = 0.8$ ),  $F$  the Coriolis frequency ( $f = 9.2 \times 10^{-5} \text{ s}^{-1}$ ) and  $\gamma$  a constant = 0.377 that they empirically derived from a series of numerical experiments. With data shown in Figure 9 we estimate  $(g'h)^2 = 0.055 \text{ m}^2/\text{s}^2$  from which the *Fong and Geyer* [2002] regression yields a fresh water transport of  $925 \text{ m}^3/\text{s}$  and similar to the transport estimates from both the moored and the shipboard data.

[26] In conclusion, three estimates of the fresh water flux in the coastal current place it in the range of  $800\text{--}1000 \text{ m}^3/\text{s}$

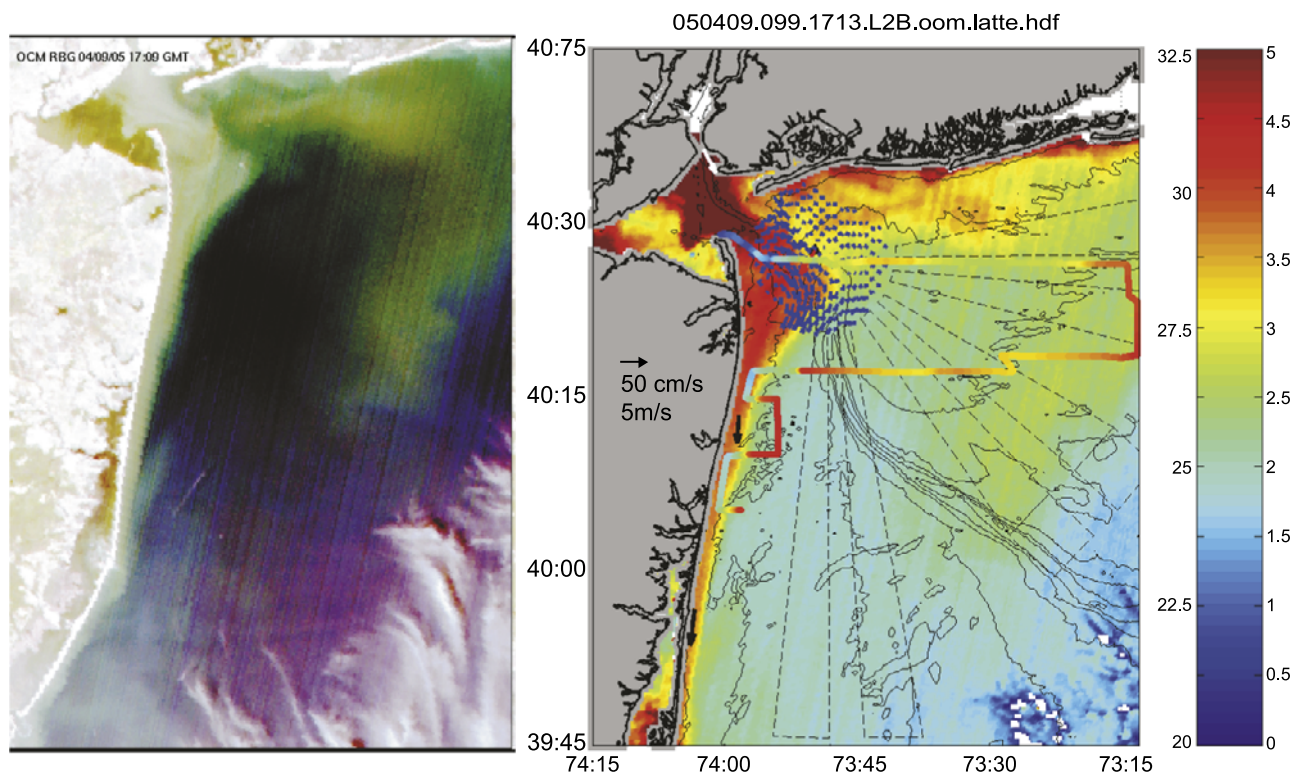


**Figure 7.** Left Panel: RGB image from Ocean sat passage on April 9th 2005 at 17:09 GMT. Right Panel: Image obtained from MODIS at 17:13 GMT. Blue arrows show CODAR field, black from shelf moorings, white from NOAA mooring at the Narrows and red vector represents winds from Ambrose. Color bar is for surface salinity from shiptrack shown in figure. Data from the transect just south of the central mooring array is used to estimate fresh water flux and shown in Figure 10. All current data has been lowpass filtered. Color map on left panel shows absorption at 488 nm and the color scale is relative with red representing high absorption and blue low absorption.

and significantly less than both the gauged fresh-water flux estimates ( $2000 \text{ m}^3/\text{s}$ ) and the Poughkeepsie estimates ( $2300 \text{ m}^3/\text{s}$ ). Consequently, the fraction of fresh water entering the coastal current appears to be only 40–50% of the fresh water that exits the estuary and the remaining freshwater goes into bulge formation. Given the estimate of the Rossby number of the outflow (0.3–0.5) our estimate of the fraction of fresh water that enters the coastal current is consistent with Figure 7 in *Fong and Geyer* [2002] that indicates that for a Rossby number of 0.5 approximately  $1/2$  of the estuarine fresh-water discharge enters the coastal current and the remaining half goes into bulge growth. Furthermore, since fresh water flux in the coastal current ceased after 13 April an even larger fraction of the estuarine outflow must have ultimately gone into bulge formation. Indeed integrating the fresh water flux estimated from the mooring deployment over the entire event (8 April–15 April), and assuming a constant plume width of 4 km we estimated that  $4 \times 10^8 \text{ m}^3$  of fresh water was transported down-shelf in the coastal current. In contrast, the total fresh water discharged into the coastal ocean during this time period was  $1.3 \times 10^9 \text{ m}^3$  based on the gauged estimate and  $1.5 \times 10^9 \text{ m}^3$  using the Poughkeepsie estimate. Thus the bulk of the fresh water that exited the estuary appears not to have gone into the coastal current, but rather into formation of a bulge.

[27] Finally, we note that the rapid increase in fresh-water flux apparent in the moored data on 15–16 April, occurred in response to a predominately east wind. We suggest that the east wind drove the bulge toward the New Jersey coast and this fed the rapid increase in down-shelf fresh water flux. This is consistent both with numerical simulations [*Choi and Wilkin*, 2007] and with theoretical arguments of bulge dynamics interacting a coastal wall [*Nof and Pichevin*, 1988].

## 6. The Bulge

[28] Many aspects of the near-field structure of Hudson's outflow that we observed in April 2005 were consistent with bulge phenomenology described in laboratory experiments [*Avicola and Huq*, 2003a; *Horner-Devine et al.*, 2006]. While details of the circulation are often obscured by wind-forcing and tidal dynamics (processes not included in the laboratory experiments) the outflow tended to form a recirculation that limited the transport into the coastal currents. We note that the formation of a bulge may be influenced by both tidal and wind-forcing. For example, tides will increase the Rossby number of the outflow favoring bulge formation, and tidally driven eddies may further augment bulge formation. However, tidal mixing will also deepen the outflow and alter both the Froude and Burger numbers which are also important parameters gov-

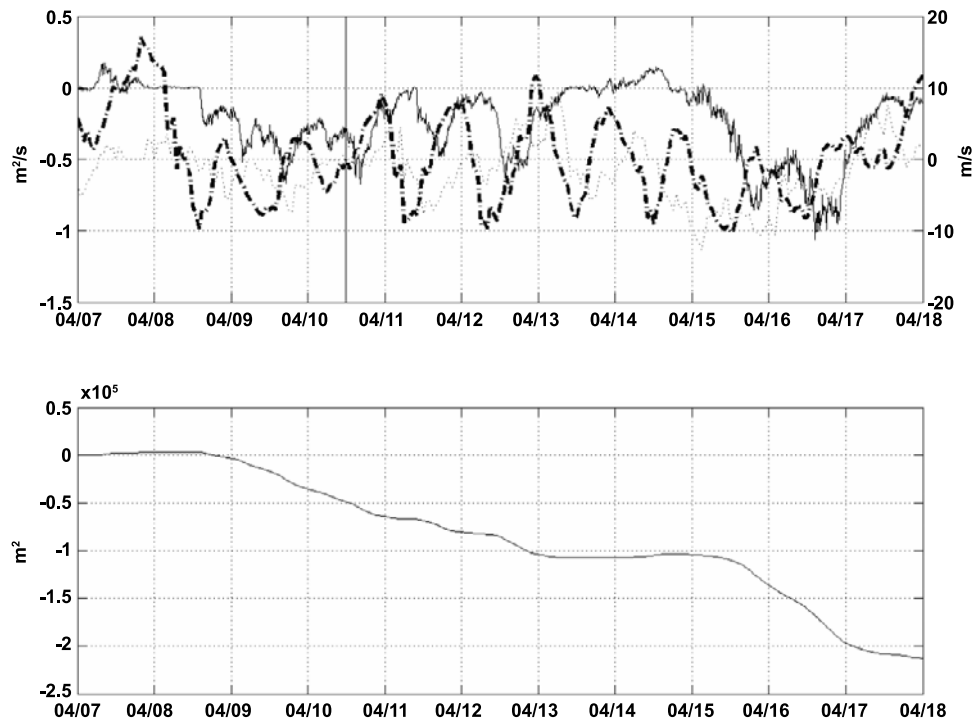


**Figure 8.** Upper panel shows fresh water flux ( $\text{m}^2/\text{s}$ ) from mooring at C1 (solid line), hourly north south (thick dashed) and east/west (thin dotted) winds from Ambrose light tower. Vertical line on 4/10 indicates time that fresh water flux was estimated with shipboard survey. Lower panel shows time integral of fresh water flux beginning on 4/7. Negative values indicate down-shelf transport.

erning bulge formation. The outflow angle which *Avicola and Huq* [2003a] suggest is the factor that determines bulge formation is strongly impacted by wind-forcing, even at the diurnal period. For example the early morning ebb at 0800 on 11 April occurred in the presence of northerly winds and drove the outflow to the south (it was into this ebb that dye was injected following the passage of the new plume) (Figure 10). In contrast the late afternoon ebb occurred in the presence of the southerly sea-breeze and deflected the outflow to the left and significantly increased the angle of the outflow. The outflow in the morning makes an angle approximately 30 degrees with the New Jersey Coast, while the late afternoon ebb makes an angle closer to 60 degrees with the coast. *Avicola and Huq* [2003a] suggested that when the outflow angle exceeded 60 degrees bulge formation was evident in their laboratory experiments.

[29] While the results of *Avicola and Huq* [2003a] suggest that the morning ebb, with its oblique outflow angle, should feed a coastal current the trajectory of drifters and dye suggested otherwise (Figure 11). Dye and drifters were released following the passage of this ebb's tidal bore. The bore was evident by a rapid increase in the velocity, deepening of the surface layer and the surface signature of trains of internal waves. Both the drifters and the dye initially headed west-southwest and veered consistently to the right. Between 2 and 3 h after release their trajectories were normal to the coast and on approaching the coast the remaining drifter (one of the drifters was removed after 3 h) and dye began to move northward. As the dye approached the coast it rapidly spread both north and south, however it

tended to move to the north over the next 48 h (Figure 11) consistent with the mean surface velocity at N1. Yet, despite the recirculation in the bulge a coastal current persisted, apparent by down-shelf currents at C1, and indicated that some of the bulge is leaking out into the coastal current. In general many aspects of the feature depicted in Figure 11 are similar to the conceptual model drawn by *Avicola and Huq* [2003a, Figure 2c]. In particular both the data and their model show a strong divergence in the along channel flow in the region between the bulge and the coastal current and this along shore divergence is maintained by a converging onshore flow.

[30] Surface chlorophyll-a maps from MODIS along with surface salinity maps and equivalent depth of fresh water maps from an 13–15 April survey show clear evidence the ballooning bulge (Figure 12). The surface map on 4/9–10 (Figure 7) shows both the old plume to the east and the development of the new plume that includes waters less than 25 psu both in the bulge and in the coastal current. While the 4/9–10 survey was too crude to estimate the fresh water volume of the bulge region we were able to estimate the fresh-water volume of the bulge region on the 4/13–15 survey.

[31] Of the 11 cross-shelf lines shown in Figure 12, we were able to estimate fresh water volume per meter of coast line for the 7 of the 8 southern lines. (The towed vehicle had to be pulled while on line 8 after its cable was snagged by fishing gear). Line 7 has the highest fresh water content with over  $6 \times 10^4 \text{ m}^2$  of fresh water per unit meter of coast line, and presumably the fresh water content increases

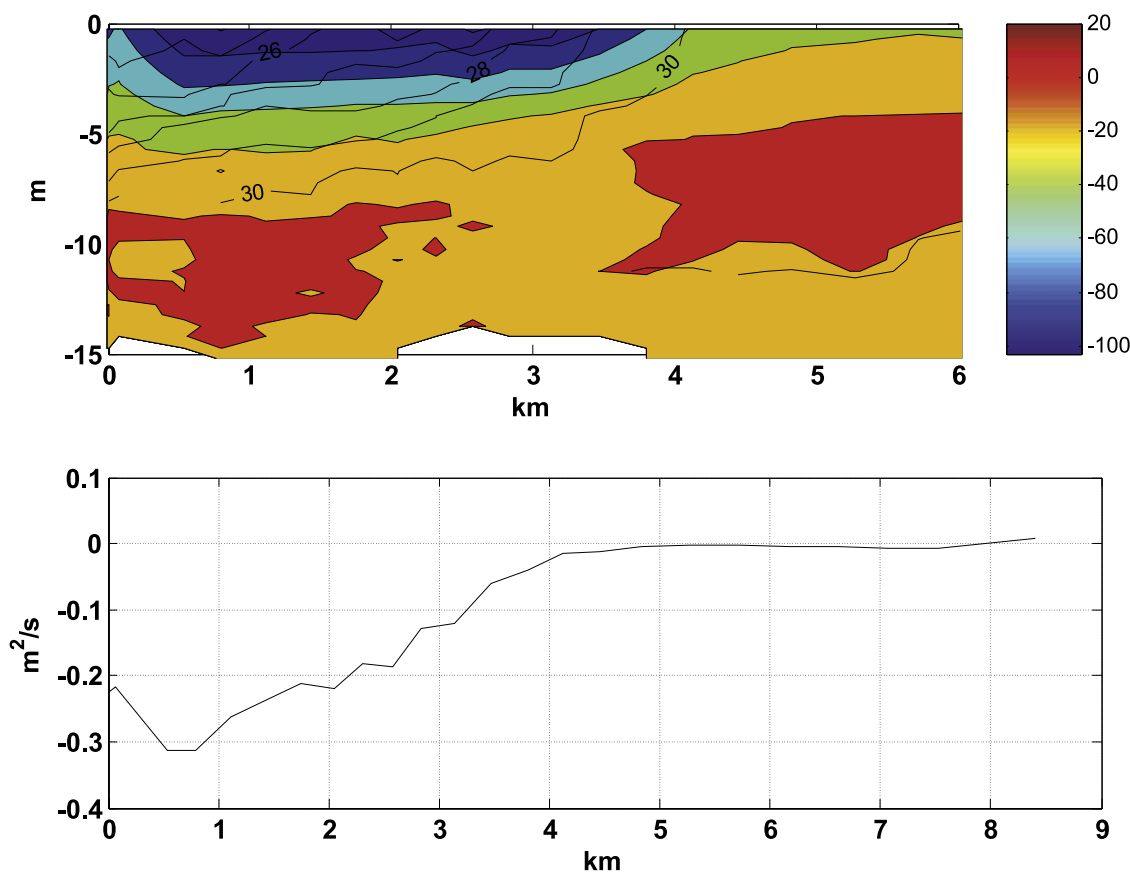


**Figure 9.** Upper panel: along shore velocity (color) and salinity (contour) from crossing of plume on April 10th just south of mooring array (ship track shown in Figure 7). Negative currents are down shelf. Currents above 3 meter below the surface are linearly extrapolated. Lower panel: Fresh water flux per meter based on data shown in upper panel.

moving northward. Fresh-water volumes reduced to  $4\text{--}5 \times 10^4 \text{ m}^3$  per unit meter of coast line on the southern 4 lines. On the 3 northern lines the bulk of the fresh water is incorporated in the bulge region, while for the southern 4 lines fresh water is evenly split between the fresh water along the coast, and the old plume in the vicinity of the shelf valley. Using a value of  $5 \times 10^4 \text{ m}^3$  to represent the fresh water per meter content of the bulge suggests that the 40 km long bulge contains  $2 \times 10^9 \text{ m}^3$  of fresh water. Note that this fresh water inventory exceeds both the gauged and Poughkeepsie estimate of the total fresh water supplied by the rivers between April 8th, when this bulge was formed and 15 April when we completed our survey. While the fresh water inventory in the bulge must be less than what was discharged because a portion was advected away in the coastal current we also recognize the estimate of fresh water volume in the bulge is crude. However, the lag between upland discharge of fresh water into the river at the gauges and outflow flow at the Narrows suggests that the freshwater content of the bulge should be compared to a discharge record that is lagged by a few days, and since the discharge was rapidly dropping during this event this would increase the amount of fresh water delivered to the coastal ocean during this event. In fact a 3 day lag yields the volume of fresh water delivered to the ocean during this event of  $1.9 \times 10^9 \text{ m}^3$  based on the gauged data and  $2.1 \times 10^9 \text{ m}^3$  based

on the Poughkeepsie data. Regardless of the details, however, it is clear that the bulk of the freshwater discharged into the coastal ocean during this event went into bulge formation rather than the coastal current.

## 7. Shelf Wide Implications

[32] The tendency for the Hudson's outflow to form a bulge has important implications on cross-shelf transport processes because once the fresh water is away from the coast its fate is determined by wind-forcing and ambient shelf circulation, rather than being self-advected away in a narrow coastal current. The bulge formation tends to place water in the vicinity of the shelf-valley and over the 40–50 m deep isobath. It is between these isobaths where the fresh water moving offshore in Figure 12 resides. While details of the ambient shelf flows are beyond the scope of this paper, several other studies have suggested that frontal systems reside between the 40–60 m isobaths in the New York Bight [Biscaye *et al.*, 1994; Bumpus, 1973; Ullman and Cornillon, 1999]. Frontal structure along this isobath appears to be associated with a surface convergence in the vicinity of the 50 m isobath associated with a mean cross-shelf flow characterized by upwelling inshore of this isobath with a downwelling circulation seaward. Cross-shelf transport pathways along the 40–50 m isobath, just west of the

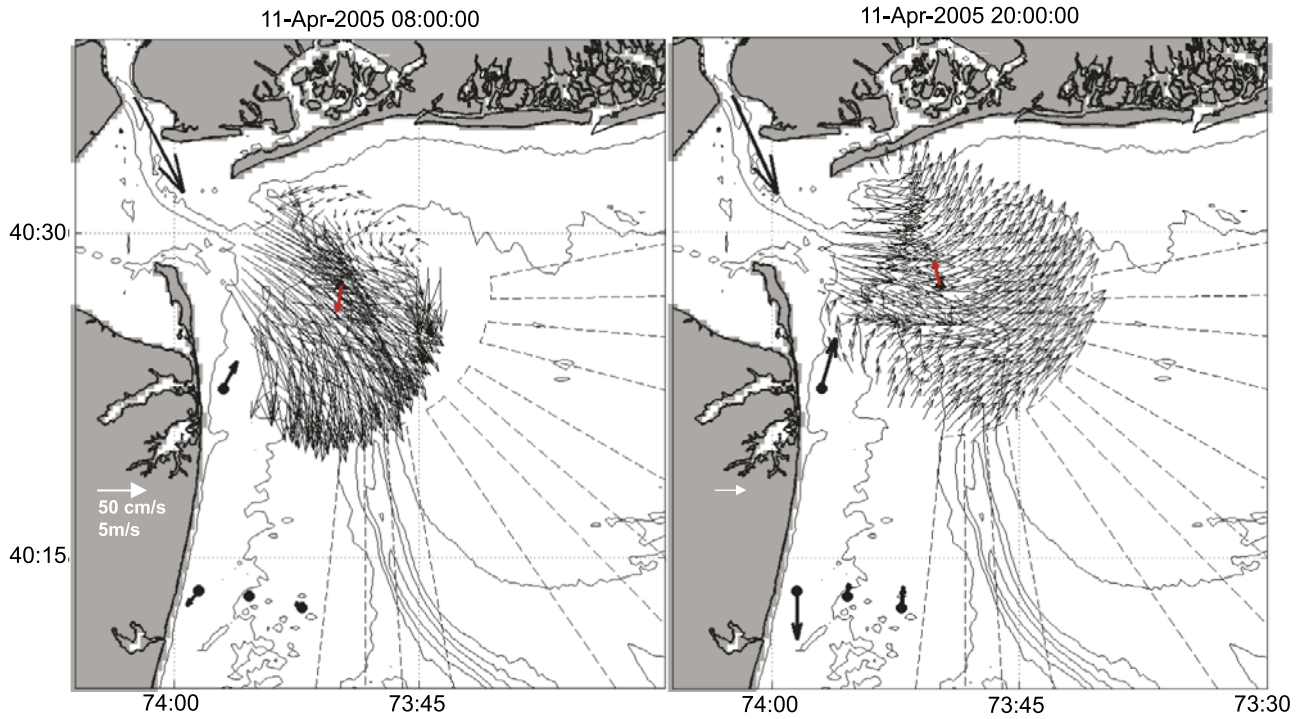


**Figure 10.** Surface currents (black vectors) and winds (red) during subsequent ebb tides on April 11th. Isobaths are contoured at 10 m intervals.

050411.101.1713.L2B.oom.latte.hdf

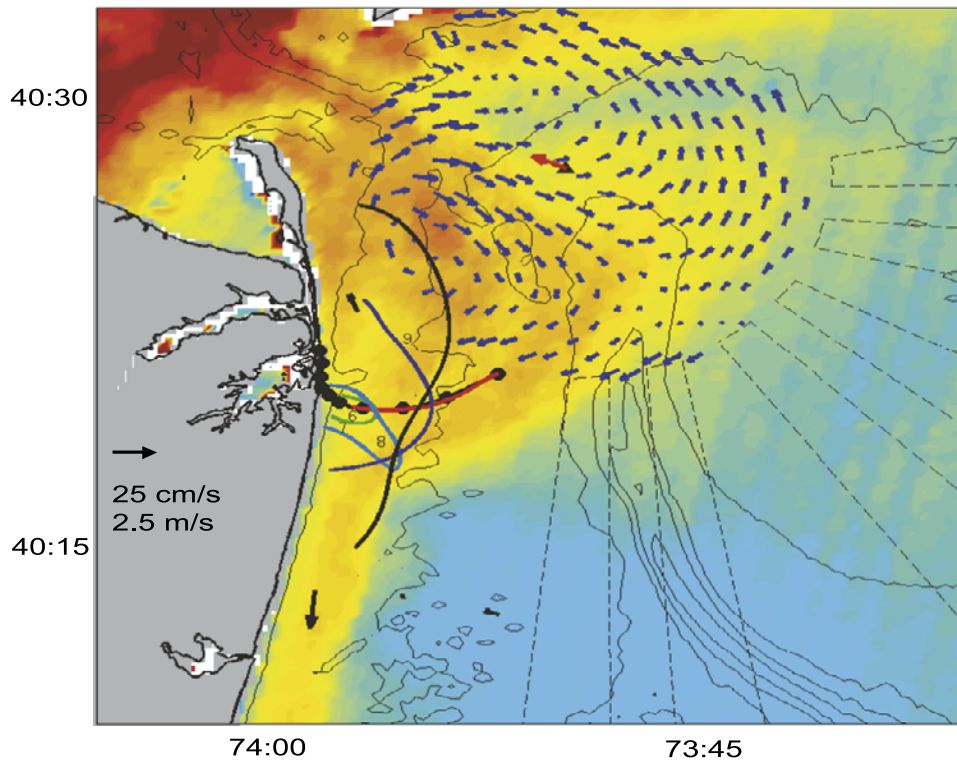


**Figure 11.** Ocean color from OCM, low-pass filtered surface currents from CODAR and mooring array. Red line shows drifter trajectory with black dots plotted each hour. The drifter was deployed during the time of the dye injection. Numbers indicate approximate location of center of dye patch and lines the approximate extent of the patch for surveys 6–9. These surveys occurred 4.3, 8.4 12.2 and 18 hours after injection respectively.

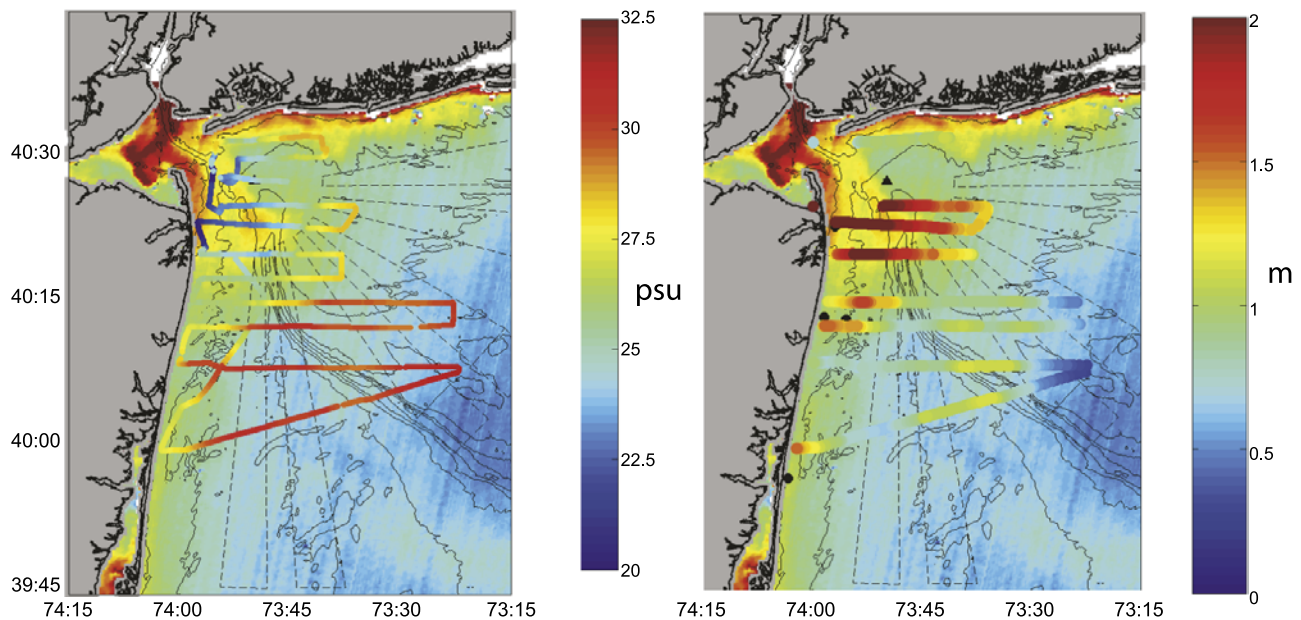


**Figure 12.** Both panels show OCM derived chlorophyll-a surface concentration from April 13th 17:13 GMT. In both panels the color scale for chlorophyll-a is relative with red representing high concentrations and blue low concentrations. The right panel shows surface salinity and the left panel shows equivalent fresh water in meters based on a reference salinity of 32 psu. The color bar is scaled to these variables shown on the shiptrack. The survey began on April 13th at 10:45 GMT and ended April 15th at 0500 GMT. Ship traces that show surface salinity but not equivalent fresh water are during times that the towed vehicle was either out of the water or held at the surface.

shelf valley, are evident in long term mean surface currents from long range CODAR data (personnel communications Scott Glenn, Josh Kohut) and appear to be correlated with upwelling winds that persists for one week or more (Castelao et al., Cross-shelf transport of fresh water in the New Jersey Shelf during Spring and Summer 2006, submitted to *Journal of Geophysical Research*). It was over these isobaths that we observed significant fresh-water on the south-eastern reaches of the survey shown in Figure 12. We note that this fresh water exited the estuary around 6 April was driven along the Long Island Coast by upwelling favorable winds on 6–8 April and subsequently drifted south during the next 5 days when winds were dominated by strong diurnal variability but weak daily means (Figure 6).

[33] Evidence of rapid cross-shelf transport of fresh water is apparent in Glider data obtained along the Rutgers University’s Endurance line that lies approximately 100 km south of the Hudson’s outflow (Figure 13–Figure 14). Comparison between a section run before the freshet (10–16 March) and one run 6 weeks after the freshet (17–24 May) shows significant freshening across the entire 150 km wide shelf (Figure 13). The May section shows that, with the exception of the intrusion of warm/saline slope waters at the end of the section, the entire shelf has freshening by approximately 1psu or more. We note that the surface salinity front located near 74 35 W coincides with a temperature front that AVHRR imagery reveals extends along much of the 100 km long NJ shelf (Figure 14). Estimates of the fresh water content based on the May glider section are  $1.2 \times 10^5$  m<sup>2</sup> of fresh water per meter of coast line. Assuming that the along shore extent of this

feature is 100 km the fresh water content on the shelf is  $12 \times 10^9$  m<sup>3</sup> and approximately equal to our estimates of the total fresh water discharged into the coastal ocean since the onset of the freshet between 1 March and 15 May, with the both the “gauged” and “Poughkeepsie” estimates of total discharge over this period equal to  $10 \times 10^9$  m<sup>3</sup>.

[34] The cross-shelf mixing of the spring freshet by early summer is consistent with results of *Mountain* [2003] who analyzed two decades of hydrographic data along from Cape Hatteras, North Carolina to Nantucket Shoals. *Mountain* noted that while there was a strong seasonal signal to mean shelf salinity in the New York Bight Apex, seasonal variability in salinity was not detectible to the south off of Delaware and Chesapeake Bays. We suggest that because these latter two systems form coastal currents fresh water tends to be trapped along the coast and was not resolved by the spatially coarse surveys they analyzed. In contrast, the rapid cross-shelf mixing of the Hudson plume would have been more readily resolved by those surveys.

## 8. Conclusions

[35] A suite of observations indicate that the Hudson’s outflow is susceptible to bulge formation under high discharge conditions. This tends to limit fresh water transport in the nearshore coastal current and enhance cross-shelf transport to mid-shelf. Even during a period of downwelling favorable winds the fresh-water transport in the coastal current was less than 1/2 of the estuarine freshwater outflow. The tendency for a major fraction of the outflow to go into unsteady bulge formation, rather than coastal

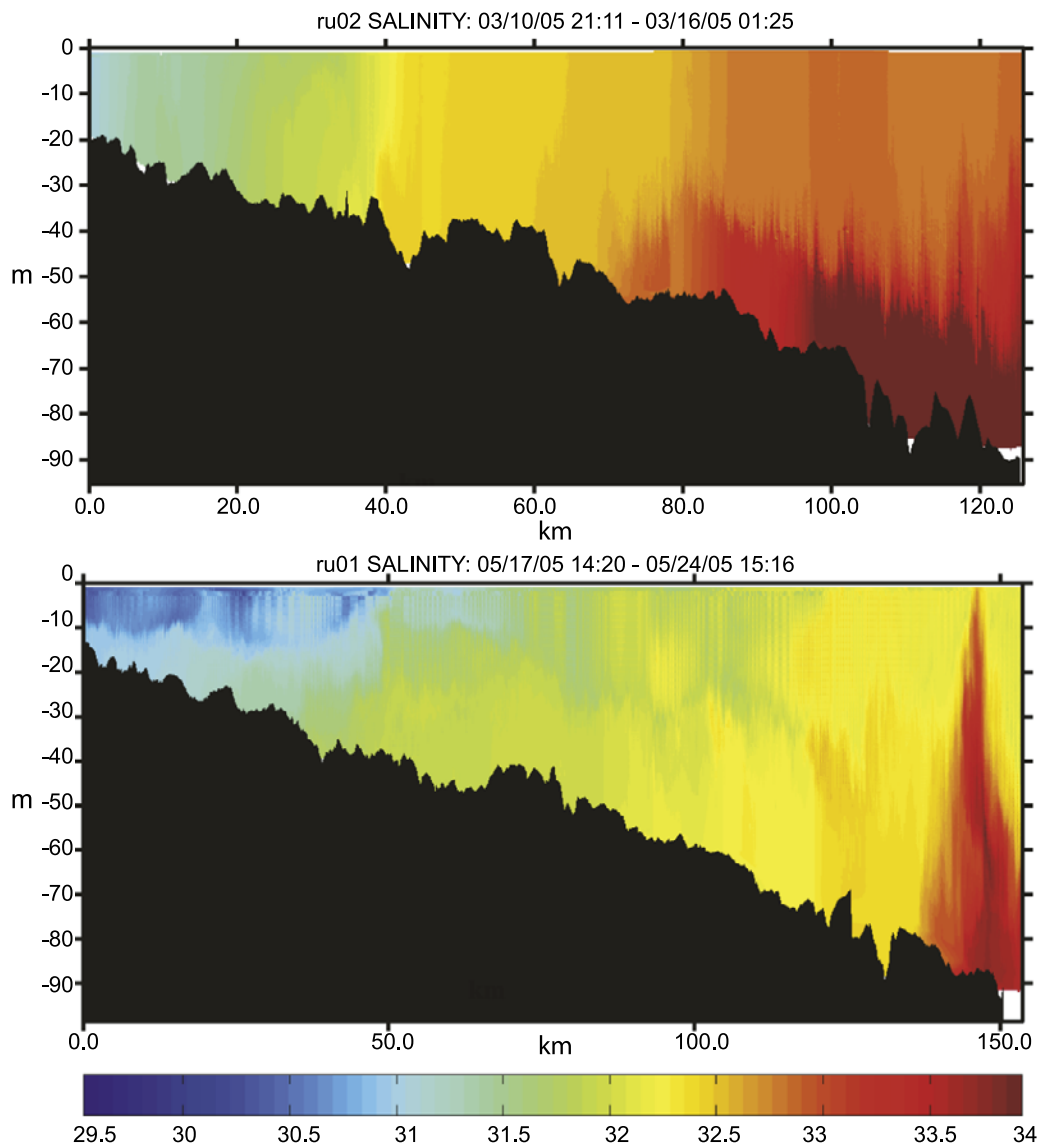


**Figure 13.** Cross-shelf sections of salinity from glider sections run on March 10–16, 2005 (upper panel) and May 17–24, 2005 (lower panel). The colorbar is practical salinity units. The glider transect is shown in Figure 14.

current is consistent with theoretical [Nof and Pichevin, 1988], laboratory [Avicola and Huq, 2003b; Horner-Devine *et al.*, 2006] and numerical studies [Fong and Geyer, 2002] of buoyant discharges. The outflow's trajectory was also highly sensitive to wind-forcing even in the diurnal band and this may have enhanced bulge recirculation as suggested by mechanism proposed by Avicola and Huq [2003b]. Transport in the coastal current is suggestive of a geostrophic cross-shore momentum balance, similar to other coastal sites [Lentz *et al.*, 1999] and modeling studies [Fong and Geyer, 2002].

[36] The tendency for the Hudson's outflow to generate a bulge may be due to several factors. First, there is a tendency for the outflow to make a large angle with the coast line, which laboratory experiments by [Avicola and Huq, 2003a; Horner-Devine *et al.*, 2006] suggest will favor bulge formation. Secondly, unlike the Chesapeake and Delaware the Hudson's outflow is not along a straight

coastline but rather into an Apex. The mean down-shelf circulation probably does not extend into this corner and thus there is not an ambient flow that tends to pin the outflow to the coast. Thirdly, there is no bathymetric channel to steer Hudson's outflow toward the coast, as there is in the Chesapeake's outflow [Valle-Levinson *et al.*, 2007]. Finally, the observations presented in this paper occurred following a large discharge event which may favor bulge formation as suggested by Choi and Wilkin [2007] relative to times of lower discharge events where presumably, in the absence of winds, a larger fraction of the outflow would go into the coastal current.

[37] Finally the tendency for the Hudson's outflow to form a bulge during times of high river discharge has significant implications for biogeochemical pathways. Rather than material being rapidly advected away in a coastal current material in the estuarine discharge, tends to be trapped near the outflow. Nutrient uptake and primary

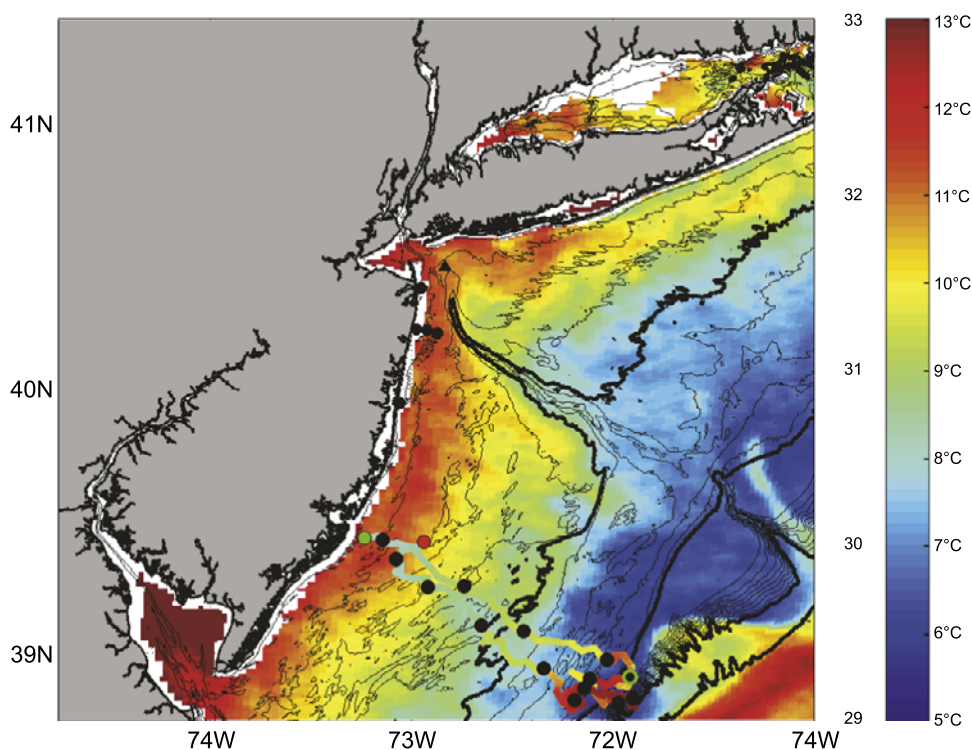


**Figure 14.** Sea Surface temperature from AVHRR at 14:55 on May 29th 2005 along with surface salinity from glider deployment from May 17th–June 11th. Colorbar is labeled for temperature (on the right) and salinity (on the left). Thick contours are used for the 50, 100, 1000 and 2000 meter isobath. Green and red dots mark the beginning and end of the glider deployment on May 17th 14:20 and June 11th 14:50 respectively. Solid black dots on glider track mark two day intervals. Black dot with green circle marks glider location at the time of the satellite pass.

production was so rapid in this region (Schofield et al., “The Hudson River Plume and its role in low dissolved Oxygen in the Mid-Atlantic Bight” submitted to *Journal of Geophysical Research*) that by the time the outflow reached the coastal current primary production was nutrient limited and rapid blooms in the bulge quickly crashed and settled to the bottom and lowered dissolved oxygen levels in the lower layer. Furthermore, the temporary retention of material in the apex region also appears to impact the fate and transport of contaminant metals (Reinfelder et al., in prep). Thus material that is rapidly cycled in the plume may quickly settle out into the lower layer where it may be transported back into the estuary by the landward flowing lower layer and increase the trapping efficiency of the estuary. On the other hand, material that remains dissolved in the plume for weeks appears to be rapidly mixed across the shelf. Details on the biogeochemical implications of the results presented in this paper will be featured in a series of interdisciplinary papers based on the LaTTE program.

[38] **Acknowledgments.** We thank two anonymous reviewers for their comments. We thank the Crew and Captains of the Cape Hatteras and the Oceanus for their efforts and the crew at Millers Launch. We also thank the dedicated members of RU COOL, with particular gratitude to Chip Haldeman who led the mooring deployment and served many roles on the Oceanus. The Observatory was supported by the Office of Naval Research, The National Science Foundation, the National Ocean Partner Program, the National Oceanic and Atmospheric Administration, the Department of Homeland Security, the Department of Defense, the Envi-

ronmental Protection Agency and the National Aeronautic and Space Administration. This study was supported by the National Science Foundation through grant OCE-0238957.

## References

- Abood, K. A. (1977), Evaluation of the circulation in partially stratified estuaries as typified by the Hudson River, Ph. D. Thesis, Rutgers University.
- Avicola, G., and P. Huq (2003a), The characteristics of recirculating bulge region in coastal buoyant outflows, *J. Mar. Res.*, *61*, 435–463.
- Avicola, G., and P. Huq (2003b), The role of outflow geometry in the formation of the recirculating bulge region in coastal buoyant outflows, *J. Mar. Res.*, *61*(4), 411–434.
- Biscaye, P. C., C. N. Flagg, and P. G. Falkowski (1994), The Shelf Edge Exchange Processes experiment, SEEP-II: An introduction to hypotheses, results and conclusions, *Deep-Sea Res.*, *41*, 231–252.
- Bumpus, D. F. (1973), A description of the circulation on the continental shelf of the east coast of the United States, *Progr. Oceanogr.*, *6*, 111–157.
- Chapman, D. C., and S. J. Lentz (1994), Trapping of a coastal density front by the bottom boundary layer, *J. Phys. Oceanogr.*, *24*, 1464–1479.
- Choi, B. J., and J. L. Wilkin (2007), The effect of wind on the dispersal of the Hudson River plume, *J. Phys. Oceanogr.*, *37*(7), 1878–1897.
- Fong, D. A., and W. R. Geyer (2001), Response of a river plume during an upwelling favorable wind event, *J. Geophys. Res.*, *106*, 1067–1084.
- Fong, D., and W. R. Geyer (2002), The alongshore transport of freshwater in a surface-trapped river plume, *J. Phys. Oceanogr.*, *32*, 957–972.
- Garvine, R. (1999), Penetration of buoyant coastal discharge onto the continental shelf: A numerical model experiment, *J. Physical*, *29*, 1892–1909.
- Glenn, S. M., and O. Schofield (2004), Observing the oceans from the COOLroom: Our history, experience, *Oceanography*, *16*.
- Harris, C. K., B. Butman, and P. Traykovski (2003), Winter-time circulation and sediment transport in the Hudson Shelf Valley, *Cont. Shelf Res.*, *23*, 801–820.
- Horner-Devine, A. R., D. A. Fong, S. G. Monismith, and T. Maxworthy (2006), Laboratory experiments simulating a coastal river outflow, *J. Fluid*, 203–232.

- Houghton, R. W., C. E. Tilburg, and R. W. G. a. A. Fong (2004), Delaware River plume response to a strong upwelling favorable wind event, *Geophys. Res.*, *31*.
- Kohut, J. G. S. M., and D. Barrick (2001), Multiple HF-Radar system development for a regional Longterm Ecosystem Observatory in the New York Bight, *American Meteorological Society: Fifth Symposium on Integrated Observing Systems*, 4–7.
- Kohut, J., S. Glenn, and J. Paduan (2006), The inner-shelf response to tropical storm Floyd, *J. Geophys. Res.*, *111*, C09S91, doi:10.1029/2003JC002173.
- Lee, Z., K. L. Carder, and R. A. Arnone (2002), Deriving inherent optical properties from water color: A multiband quasi-analytical algorithm for optically deep waters, *Appl. Opt.*, *41*, 5755–5772.
- Lentz, S. J., and K. R. Helfrich (2002), Buoyant gravity currents along a sloping bottom in a rotating fluid, *J. Fluid Mech.*, *464*, 251–278.
- Lentz, S., R. T. Guza, S. Elgar, and F. F. a. T. H. C. Herbers (1999), Momentum balances on the North Carolina inner Shelf, *J. Geophys. Res.*, *104*, 18,205–18,226.
- Lerczak, J. A., W. R. Geyer, and R. J. Chant (2006), Mechanisms driving the time-dependent salt flux in partially stratified estuary, *J. Phys. Oceanogr.*, *36*, 2283–2298.
- Morison, J., R. Anderson, N. Larson, E. D'Asaro, and T. Boyd (1994), The correction for thermal-lag effects in sea-bird CTD data, *J. Atmos. Oceanic Technol.*, *11*, 1151–1162.
- Mountain, D. G. (2003), Variability in the properties of Shelf Water in the Middle Atlantic Bight, 1977–1999, *J. Geophys. Res.*, *108*(C1), 3014, doi:10.1029/2001JC001044.
- Newman, W. S., D. L. Thurber, H. S. Awiss, A. Rokach, and L. Musich (1969), Late Quaternary geology of the Hudson River estuary: a preliminary report., *31*, 548–570.
- Nof, D., and T. Pichevin (1988), The ballooning of outflows, *J. Phys. Oceanogr.*, *31*, 3045–3048.
- Rennie, S. E., and S. Lentz (1999), Observations of a pulsed buoyance current downstream of Chesapeake Bay, *J. Geophys. Res.*, *104*, 18,228–18,240.
- Ullman, D., and P. Cornillon (1999), Satellite-derived sea surface temperature fronts on the continental shelf off the northeast U.S. coast, *J. Geophys. Res.*, *104*.
- Valle-Levinson, A., K. Holderied, and C. L. a. R. J. Chant (2007), Subtidal flow structure at the turning region of a wide outflow plume”, *J. Geophys. Res.*, *112*, C04004, doi:10.1029/2006JC003746.
- Whitney, M. M., and R. W. Garvine (2005), Wind influences on a coastal buoyant outflow, *J. Geophys. Res.*, *110*, C03014, doi:10.1029/2003JC002261.
- Yankovsky, A., and D. C. Chapman (1997), A simple theory for the fate of buoyant coastal discharges, *J. Phys. Oceanogr.*, *27*, 1386–1401.

---

J. Bosch, R. J. Chant, S. M. Glenn, E. Hunter, J. Kohut, and O. Schofield, Institute of Marine and Coastal Studies, Rutgers University, New Brunswick, NJ, USA. (chant@marine.rutgers.edu)

R. F. Chen, University of Massachusetts Boston, MA, USA.

R. W. Houghton, Lamont-Doherty Earth Observatory, Columbia University, Palisades, NY, USA.